

## **Convection with heavy rain, 3 May 2022 in Valencia (dcmdb: Spain\_202205)**

### **Case description**

A static convective system accumulated record precipitation amounts in the Valencia area with 181 mm in Viveros, 122 in Valencia airport, 122 in Sagunto and 96 in El Puig. More information available in DE\_330\_M330.5.3.1\_202210\_MilestoneNote\_v2.

### **Model configurations:**

- Baseline simulations. HARMONIE-AROME CY46h1 including upper-air and surface DA, 7 days warmup. Runs on ECMWF-ATOS at 500 m resolution (1536x1560, 65L). Nested in IFS HRES.
- On-Demand DT prototype 0.3.0 using HARMONIE-AROME configuration based on CY46h1. Runs on ECMWF-ATOS at 500 m resolution (1536x1620, 90L). Initial and boundary conditions from IFS HRES.
- On-Demand DT prototype 0.3.0 using AROME configuration based on CY48t3.

### **Reference simulations:**

- IFS-HRES (operational version)
- HARMONIE-AROME baseline exp including

**Dates run (OD-DT):** 2022050300 to 2022050312, each 6 hours.

### **Output (OD-DT):**

- /ec/res4/scratch/esp0754/deode/CY46h1\_HARMONIE\_AROME\_M05C/
- /ec/res4/scratch/esp0754/deode/CY48t3\_AROME\_M05C/

**Observations used for spatial verification:** OPERA radar (1-hour accumulated precipitation)

**Verification/Assessment/Analysis:** The analysis of this extreme event has been focused on a fixed rectangular region with an approximate area of about 48000 km<sup>2</sup> and centered on the maximum peak of accumulated precipitation. This domain is represented by a black rectangle in Figure 1. The time interval for this analysis has been set from 17 to 23 UTC. The OPERA radar data show a static system on the coast resulting in the cumulative precipitation shown in the middle panel. On the other hand, the reference experiment (IFS-HRES, left panel) represents highly underestimated precipitation values at sea and inland, close to the event. The OD-DT represents a maximum of precipitation penetrating inland, possibly influenced by terrain orography. However, from 21 UTC onwards, it represents a static event on the coast that originates the accumulated values shown in the right panel, close to the maximum precipitation shown by the radar data. Regarding the cumulative precipitation of the event, the high resolution provides an added value with respect to the reference

experiment, mainly because of the high underestimation of the precipitation field during the extreme event but also because of the location (coast and inland).

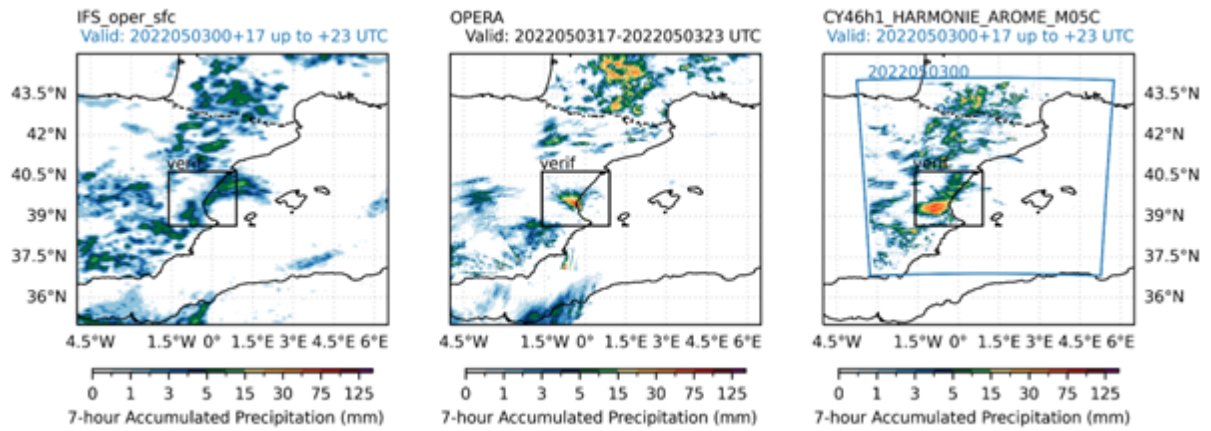


**Figure 1.** Precipitation in 7hr for IFS-HRES, OPERA radar and OD-DT (HARMONIE-AROME version). Black rectangle represents the verification domain used in the spatial verification.

In order to quantify the hourly cumulative precipitation performance of both experiments, a total of 14 time steps have been verified and compared. Figure 2 shows the Fractional Skill Score (FSS) distributions of both experiments for several hourly cumulative precipitation thresholds and spatial scales. Generally, higher spatial accuracy, i.e. higher FSS values, are obtained by the prototype. Hourly precipitation values greater than 4 mm/h are hardly found in the reference experiment due to the large underestimation of the precipitation field discussed above. This results in null FSS values obtained for IFS-HRES at all spatial scales and high thresholds. Thus, significant differences are found with the prototype for these thresholds and especially at spatial scales above 40 km. For thresholds below 4 mm/h, generally the FSS distributions of both experiments do not pass the statistical significance test but, as previously mentioned, higher FSS values are obtained with the high resolution experiment.

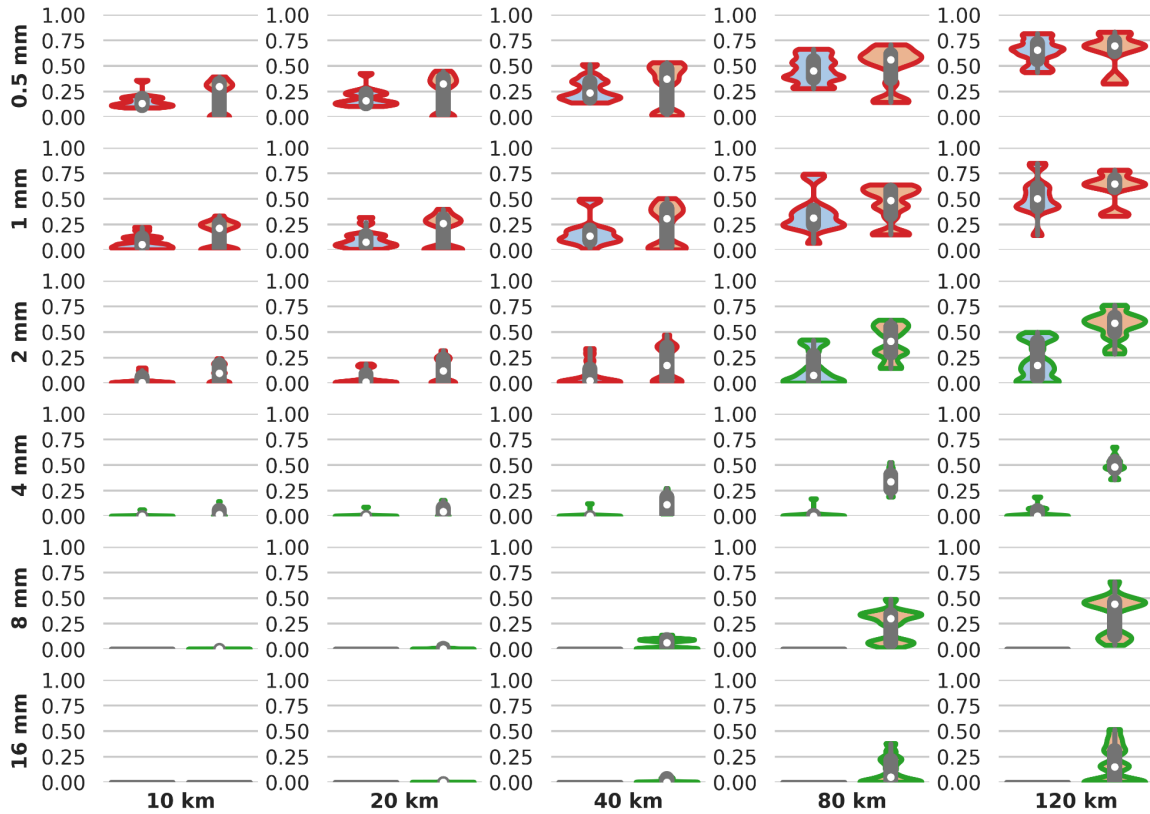


**Figure 2.** Violin plots of Fractional Skill Score (FSS) for several hourly cumulative precipitation thresholds (rows) and spatial scales (columns). Each panel shows the FSS distribution for IFS-HRES (left, blue) and OD-DT (right, orange). Green and red edges represent whether the two distributions pass the Wilcoxon signed-rank test ( $p$ -Value less than 0.05) or not, respectively.

Despite increasing the spatial scale, the FSS values do not reach values close to 1, possibly due to the bias of the precipitation values of both experiments. This can be shown by the amplitude value of the SAL plot in Figure 3. Concerning the amplitude term, the IFS-HRES precipitation field is practically unbiased because, despite the underestimation of the values, the precipitation field covers a larger extent within the verification domain, resulting in an offset of the amplitude term when compared to the high but localized precipitation values of the observations. In the prototype case, the two verified initializations are clearly differentiated. Initialization farthest from the start of the extreme event, i.e. 2022050300, overestimates the precipitation values although the extreme values (objects detected from the 97th percentile onwards) are better localized. On the other hand, the initialization closer to the event (2022050312) underestimates the precipitation field by a smaller magnitude although it is static in an inland area, more than 60 km away, resulting in values greater than 0.2 in the localization parameter. On the other hand, the extreme precipitation field values of the reference experiment are more dispersed along the verification domain (location values higher than 0.5 in some time steps). Finally, the

structure term gives us an overview about the shape of the extreme precipitation objects modeled by both experiments when compared to the observations. Higher values of this parameter are obtained for the IFS-HRES, i.e. the objects are more extensive and flatter than in the observations. A better representation of the localized precipitation of the event is represented by the prototype although the extent and shape of these extreme values is still overestimated with respect to the observations.

Taking into account all mentioned above, an added value of the high resolution is obtained when modelling the precipitation. In addition to representing the extreme values that occurred during the event, these precipitation values are better represented from the point of view of location and shape, both from a subjective analysis of the total accumulated precipitation and from the objective analysis from the FSS and SAL metrics. Similar results can be found with the AROME version of the prototype (not shown in this report).

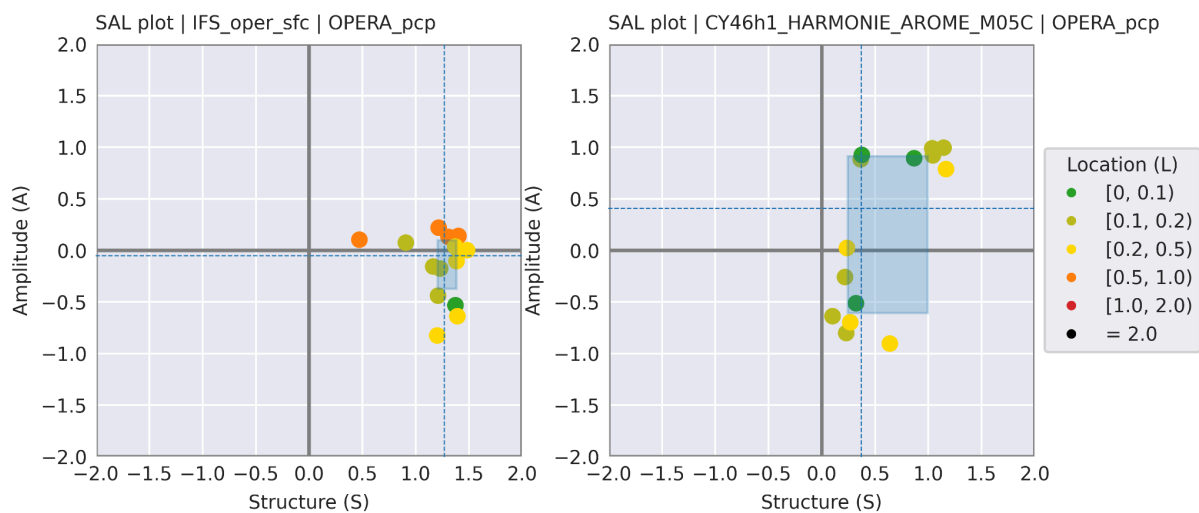


**Figure 3.** Salt plot for the IFS-HRES (left panel) and OD-DT (right panel). Each point represents a verified time step. Blue square shows the interquartile range of the amplitude and structure values contained in each of the panels. Dotted blue lines represent the median of these values.

**Sensitivity tests:** In order to analyse the added value of high resolution, two sensitivity studies have been carried out. First, the spatial verification was performed over almost the whole domain of the sub-kilometre scale experiment, i.e. not focused on the convective event. Figure 4 shows the FSS obtained by both experiments on this large verification domain. In this case, higher values are obtained by both runs, especially for scales below 40 km. The precipitation field of the reference experiment hardly presents values higher than 4 mm/h in the whole verification domain, so the results obtained are analogous to those described with the verification domain located in the extreme event (Figure 2). Very similar FSSs are obtained for thresholds below 4 mm/h, especially for the smaller scales. Although the median distributions of both experiments have close values, in general the OD-DT obtains a higher value with a smaller interquartile range, achieving a higher performance of the precipitation field. More notable differences are found in the SAL plot (Figure 5). In this

case, a larger number of objects are found within the verification domain, so the structure and location terms are modified. Also the amplitude value, as more grid cells are contained within the verification domain when computing the mean precipitation field. A great improvement in the localisation value is obtained for the reference experiment, achieving values very similar to those obtained by the DEODE prototype. However, these objects are still too large/flat, resulting in a worse structure value than the higher spatial resolution experiment. Finally, Figure 6 shows a comparison of the 3 initialisations of the OD-DT (21 verified time steps) and the base experiment at 500 m can be conducted. In this case, DA seems to be key to localize the convective event at the coast, resulting in higher FSS for all scales and thresholds even though the precipitation field is overestimated.

FSS distributions | IFS\_oper\_sfc (left) - CY46h1\_HARMONIE\_AROME\_M05C (right) | OPERA\_pcp

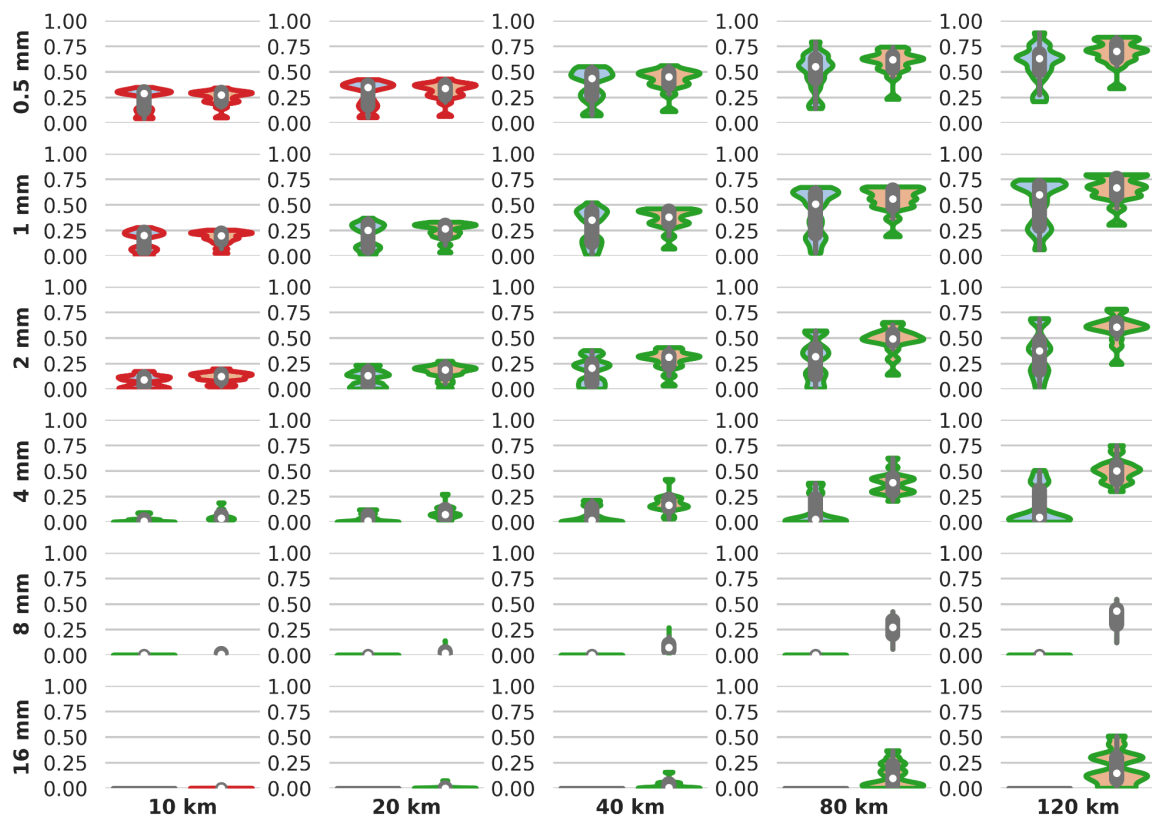


**Figure 4.** Same as Figure 2 but for a larger verification domain.

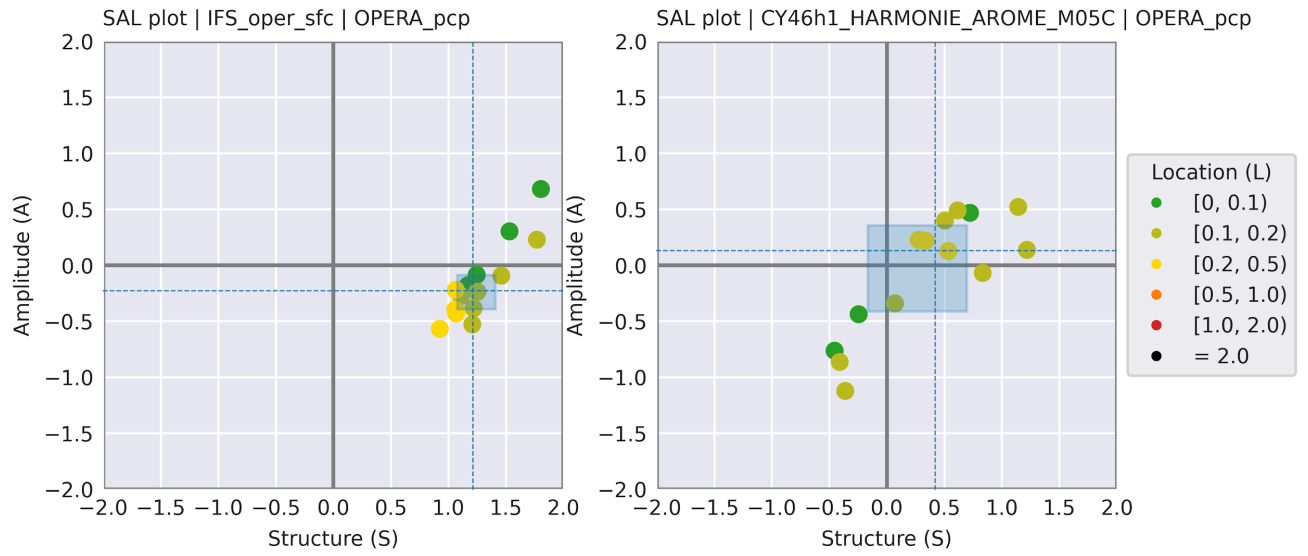


**Figure 5.** Same as Figure 3 but for a larger verification domain.

FSS distributions | VAL500m\_46h1\_de2 (left) - CY46h1\_HARMONIE\_AROME\_M05C (right) | OPERA\_pcp

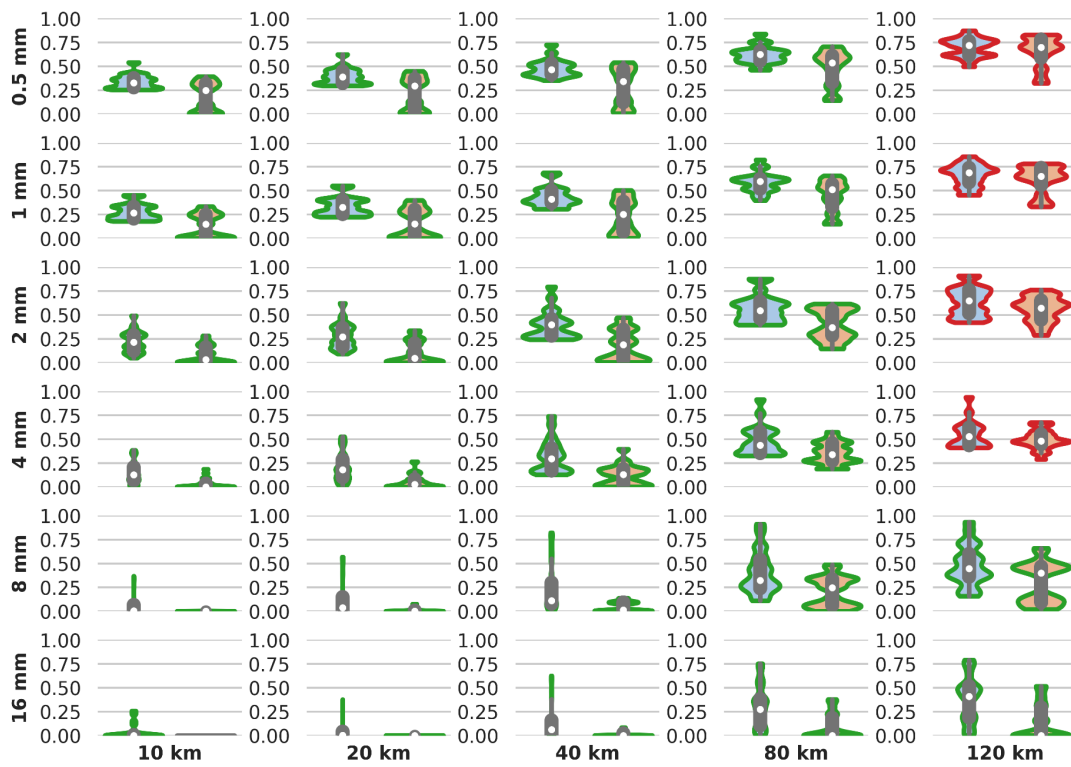


**Figure 6.** Same as Figure 2 but for 500 m spatial resolution baseline run and OD-DT.

## Conclusions

Improvement of the OD-DT in amount and location of precipitation compared to IFS-HRES although the results are far from perfect. Good candidate for testing OD-DT triggering. This type of event would benefit from including surface warmup and DA. Spatial verification is able to detect the added value of the high resolution runs].

Possible triggers:

- IFS probabilities and precipitation extremes from continuous DT (although IFS had difficulties to detect this particular case)
- Operational forecaster outlook.